Easy Access to Hydride Chemistry on a Tripodal P-Based Rhodium Scaffold

Cristina Tejel, Ana M. Geer, Sonia Jiménez, José A. López, and Miguel A. Ciriano**

Instituto de Síntesis Química y Catálisis Homogénea (ISQCH), CSIC – Universidad de Zaragoza, Departamento de Química Inorgánica, Pedro Cerbuna 12, 50009-Zaragoza (Spain)

E-mail: mciriano@unizar.es, ctejel@unizar.es

RECEIVED DATE (to be automatically inserted after your manuscript is accepted if required according to the journal that you are submitting your paper to)

ABSTRACT. The *TBPY–5* rhodium complex [(PhBP$_3$)Rh(CH$_2$=CH$_2$)(NCMe)] (**1**) {PhBP$_3$ = PhB(CH$_2$PPh$_2$)$_3$)} that contains ethylene in the equatorial plane and a labile acetonitrile ligand at one of the axial positions provides a simple entry into the chemistry of the *fac*-[P$_3$Rh] scaffold. DFT calculations using the model compound [(MeB(CH$_2$PMe$_2$)$_3$)Rh(CH$_2$=CH$_2$)(NCMe)] (**1´**) reproduce well the crystallographic geometry of **1** and converge to the isolated conformer, in which the strong π-back-donation from the metal to the π* orbital of ethylene fixes it coplanar with the equatorial plane. Oxidation of **1** is electrochemically irreversible (at 0.080 V vs. SCE), and **1** was effectively oxidized with [Cp$_2$Fe]$^+$ in acetonitrile to [(PhBP$_3$)Rh(NCMe)$_3$]$^{2+}$. Reaction of **1** with hydrogen in toluene gives the dihydride [(PhBP$_3$)Rh(H)$_2$(NCMe)] (**3**), which losses acetonitrile to give the insoluble hydride [{(PhBP$_3$)Rh(H)(μ-H)}$_2$] (**4**), while in THF with BHT (2,6-bis(1,1-dimethylethyl)-4-methylphenol) results the mixed-valence paramagnetic hydride [{(PhBP$_3$)Rh}$_2$(μ-H)$_3$] (**5**). Complexes **1** and **3** react with oxygen to give the dinuclear complex [{(PhBP$_3$)Rh(μ-O$_2$)}$_2$]. The kinetic products from the

protonation of complex **1** with carboxylic acids were found to be the ethyl complexes [($PhBP_3$)Rh(η^1-C_2H_5)(κ^2-O_2CR)] (R = Ph, Me), which establish an equilibrium in solution with the corresponding hydride complexes [($PhBP_3$)Rh(H)(κ^2-O_2CR)] (R = Ph, Me) and free ethylene. These equilibria can be shifted to the desired compound working under either an atmosphere of ethylene or vacuum. Sequential protonation of **1** and **3** with HBF_4 in acetonitrile gave cleanly the cationic hydride complex [($PhBP_3$)Rh(H)$(NCMe)_2$]BF_4 firstly and then [($PhBP_3$)Rh$(NCMe)_3$]$(BF_4)_2$ and hydrogen. Other electrophiles such as MeOTf react immediately with **1** at one phosphorus atom to give the alkylated (P–methyl) complex [{PhB(PMe)P_2}Rh(κ^2-O_2SOCF_3)].

Introduction

Metal-multipodal ligand scaffolds provide a common way to study reactions under well defined yet unusual and reactive geometries. Trofimenko's scorpionates [or tris(pyrazolyl)borate (Tp) ligands] are a classic example of such highly ordered and sterically encumbered multidentate scaffolds.[1] The success of tris(pyrazolyl)borates has inspired the development of new anionic scorpionate ligands based on other donor groups that provide a facial array of [X_3] donors and differ in their topology, flexibility, and donor properties.[2] In this respect, interest has increased in anionic [P_3] donor ligands, firstly reported in 1999, which are strongly donating scorpionates. The simplest, $[PhB(CH_2PPh_2)_3]^-$ (henceforth referred to as $PhBP_3$),[3] has been shown to be suitable for creating pseudotetrahedral[4] metal environments and for stabilizing terminal imido complexes of first row late transition metals (LTM) with robust M≡NR (M = Fe, Co) triple bonds,[5] as well as unusual peroxo and hydroperoxo rhodium compounds,[6] or isocarbonyl nickel complexes.[7] Evidence for its ability to form reactive iridium complexes has been verified by C–H[8] and double geminal Si–H and Ge–H bond activation processes,[3a,9] as well as facile heterolytic hydrogen activation by nitride and hydrogenolysis by imido iron complexes, respectively, under mild conditions.[10] Substitution of the phenyl groups in $PhBP_3$ by the more basic and bulkier ^{i}Pr groups produces $[PhB(CH_2P^iPr_2)_3]^-$ ($PhBP'_3$), which subtly governs the reactivity of metals in its complexes allowing, for example, the stabilization of η^3-silane adducts of iron(II),[11] or promoting Si–H and B–C

activation processes if coordinated to iridium.[12] Moreover, bound to iron it provides support enough to accommodate this metal in an unusual wide range of oxidation states [from Fe(0) to Fe(IV)].[13] Furthermore, pseudotetrahedral manganese complexes[14] or novel dinitrogen activation chemistry has been achieved with iron and cobalt complexes.[13b] Related hybrid scorpionate ligands such as $[PhB(CH_2P^iPr_2)_2(Pz)]^-$ (PhBNP'$_2$) or $[allylB(CH_2PPh)(Pz)_2]^-$ (ABPN$_2$) stabilize terminal iron(IV) imides[15] and show new coordination modes,[16] respectively.

The utility of complexes of late transition metals with these type of ligands in catalysis remained undocumented until the use of $[(PhBP'_3)Fe(H)_3(PR_3)]$ (R = Me, Et) as catalyst precursors for olefin hydrogenation.[17] More recently, we have reported the complexes $[(PhBP_3)Rh(cod)]$ and $[\{(PhBP_3)Ru(\mu\text{-}Cl)\}_2]$[18] as pre-catalysts for the selective hydrogenation of the carbonyl group in α,β-unsaturated substrates,[19] while the cationic ruthenium complex $[(PhBP_3)Ru(NCMe)_3]PF_6$ is a catalyst precursor for hydrogen transfer reactions from 2-propanol to aromatic and aliphatic ketones.[20] Moreover, we have shown that the dihydridorhodium(III) complex $[(PhBP_3)Rh(H)_2(NCMe)]$ is an extremely efficient catalyst for the dimerisation of both, aliphatic and aromatic, enolizable and non-enolizable aldehydes under exceptionally smooth conditions.[21] Key steps in the catalytic cycle are an easy *β*-hydride insertion into the C=O bond of the aldehyde to give an alkoxide, followed by nucleophilic attack on a new molecule of coordinated aldehyde and a *β*-hydrogen elimination from the hemiacetal intermediate to regenerate the catalyst. From our experience, it was apparent that hydrogenation of carbonyl groups was preferred over C=C bonds. This prompted us to study some basic chemistry of hydride/olefin complexes on the '$(PhBP_3)Rh$' scaffold. In particular, we succeed in preparing the monoolefin complex $[(PhBP_3)Rh(C_2H_4)(NCMe)]$ (**1**), which possesses a simple olefin and a labile acetonitrile ligand, as a key compound to enter this chemistry. Herein, we report the synthesis and full characterization of complex **1**, its reactions leading to hydride and alkyl complexes and their interplay as well as other related reactions.

Results and Discussion

Synthesis and characterization of [($PhBP_3$)Rh(CH_2=CH_2)(NCMe)] (1). Reaction of [{Rh(μ-Cl)(C_2H_4)$_2$}$_2$] with [Li(tmen)][$PhBP_3$] (tmen = *N,N,N',N'*-tetramethylethane-1,2-diamine, $PhBP_3$ = $PhB(CH_2PPh_2)_3$) in acetonitrile gives the mononuclear compound [($PhBP_3$)Rh(CH_2=CH_2)(NCMe)] (**1**) as the result of the coordination of the anionic tripodal $[PhBP_3]^-$ ligand to rhodium and the replacement of one molecule of ethylene by acetonitrile. Complex **1** was isolated as an air-sensitive yellow-orange crystalline solid in good yield and fully characterized by analytical and spectroscopic methods. The isolated crystals usually contain acetonitrile of crystallization. The X-ray structure of **1** (Figure 1) shows a pentacoordinated rhodium center *fac*-bound to the three phosphorus atoms of the anion $[PhBP_3]^-$ and to ethylene and acetonitrile ligands. The geometry around the rhodium atom can be described as distorted trigonal bipyramid (*TBPY–5*) with P1 and acetonitrile at the apical positions and two P atoms (P2 and P3) and ethylene at the equatorial plane forming P–Rh–P angles close to 90° (see Table 1), i.e., smaller than the expected probably due to geometrical requirements of the tripodal ligand.

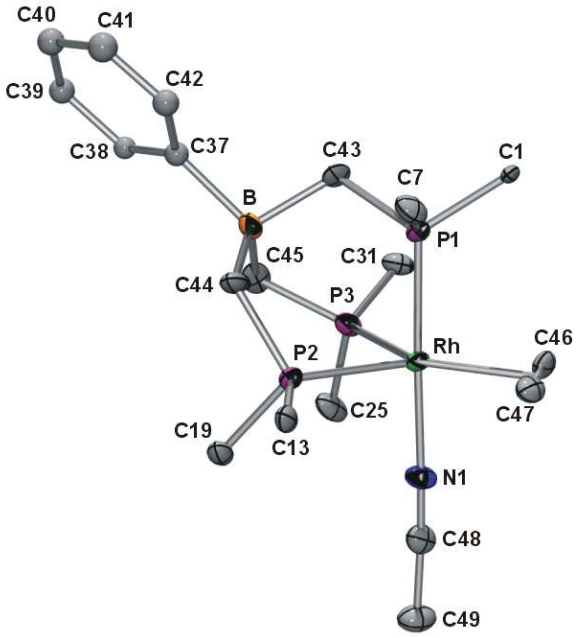

Figure 1. Structure (ORTEP at 50% level) of complex **1** (hydrogen atoms have been omitted, and only the *ipso* carbons of the phenyl groups are shown for clarity).

The Rh–P bond distances are in the normal range, with that of phosphorus at the apical position (Rh–P1) being the shortest. The ethylene molecule is coplanar to the equatorial plane [the maximum deviation of the plane defined by C46, C47, Rh, P1 and P3 is 0.012 Å], and shows a quite long carbon–carbon distance (1.443(7) Å), which indicates a strong π-back-donation from the metal to the π* orbital of ethylene.

Table 1. Selected crystallographic (complex **1**) and DFT-calculated (complex **1'**) bond distances (Å) and angles (º).

Distances	**1**	**1'**	Angles	**1**	**1'**
Rh–P1	2.2518(17)	2.303	P1–Rh–N1	178.28(15)	178.1
Rh–P2	2.3854(17)	2.445	P1–Rh–P2	88.13(6)	86.9
Rh–P3	2.3766(16)	2.448	P1–Rh–P3	89.67(6)	88.2
Rh–N1	2.060(5)	2.098	P1–Rh–Ct	93.43(16)	93.5
Rh–C46	2.139(5)	2.175	P2–Rh–P3	89.20(6)	90.2
Rh–C47	2.167(6)	2.181	P2–Rh–Ct	137.83(15)	137.7
Rh–Ct	2.029(5)	2.058	P3–Rh–Ct	132.91(15)	132.0
C46–C47	1.443(7)	1.429	N1–Rh–Ct	84.9(2)	86.3

Ct represents the middle point of C46 and C47.

The DFT (b3-lyp, LanL2DZ and 6-31G**) optimized geometry of **1** using the model compound [($MeBP_3$)Rh(CH_2=CH_2)(NCMe)] [**1´,** $MeBP_3$ = $MeB(CH_2PMe_2)_3$] reproduces well the crystallographic data (Table 1) with bond distances and angles close to those found for **1**. The experimental metal–ligand distances are slightly shorter than those from the DFT geometry, which is quite common for the b3-lyp functional. The HOMO of **1'** (Figure 2) clearly shows the bonding interaction between the π* orbital of ethylene and the d_{xy} orbital of rhodium, being this interaction responsible of the coplanar disposition of the ethylene ligand above mentioned. Attempts to model the conformational isomer having apical ethylene and equatorial acetonitrile did not reach an energy minimum, since the back-donation is maximal at the equatorial plane in a d^8-ML_5 *TBPY–5* geometry and the best π-acceptor ligands occupy

these positions. The calculations converge to the isolated conformer, which in turn represents the thermodynamically most stable conformer of complex **1**. Similarly, the conformational isomer with the ethylene molecule perpendicular to the equatorial plane does not reach any energy minimum and again converge to **1**, with ethylene coplanar to this plane.

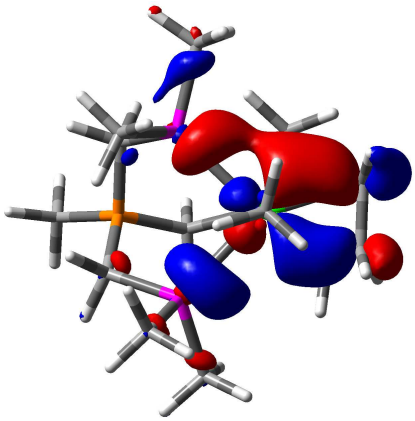

Figure 2. DFT calculated HOMO of **1**'.

Solutions of **1** in CD_2Cl_2 at –50 ºC showed well defined ^1H and $^{31}P\{^1H\}$ NMR spectra. The two equatorial phosphorus nuclei become equivalent by a symmetry plane, giving a doublet of doublets while the axial one gives a doublet of triplets in the $^{31}P\{^1H\}$ NMR spectrum. Notice that an easy turnstile motion between the two *TBPY-5* conformers (with ethylene or acetonitrile at the apical position) would produce only a doublet in the $^{31}P\{^1H\}$ NMR spectrum. The ethylene protons gave two signals in the ^1H NMR spectrum, which correspond to a non-rotating ethylene ligand, as expected from the strong π–interaction with the metal described above. On cooling, broadening of the phosphorus nuclei signals was observed and that corresponding to the equatorial ones eventually splits into two broad resonances at –90 ºC (see Supporting Information). This can be due to one or both of the following processes: i) a freezing of the free-rotation of the phenyl rings of the phosphorus atoms, in particular those at the apical position, and ii) a lack of flexibility of the framework of bonds made by the methylene carbons in $[PhB(CH_2PPh_2)_3]^-$. Both produce the loss of the mentioned symmetry plane that makes equivalent the equatorial phosphorus nuclei, and consequently, the corresponding signal splits into two ones while that of the axial phosphorus remains almost unchanged. However, the 1H NMR at

low temperature is inconclusive because broad signals for the phenyl and ethylene protons are observed. In addition, the frozen structure of the complex shows a helical disposition of the three arms of the $[PhBP_3]^-$ ligand close to a local C_3 symmetry (see Figure 3). At room temperature, broadening of the $^{31}P\{^1H\}$ NMR signals was observed at the same time that the signals of free and coordinated acetonitrile (at δ 1.97 and 1.38 ppm, respectively) become a single resonance in the ^1H NMR spectrum, which indicates that the fluxionality observed at room temperature is most probably due to dissociation/association of acetonitrile

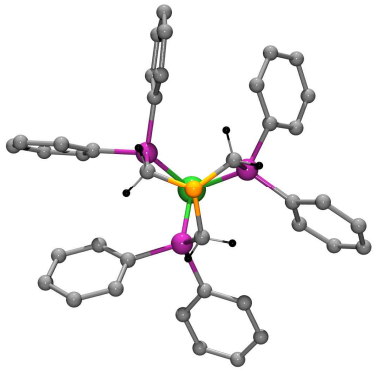

Figure 3. View of the '$(PhBP_3)Rh$' fragment of **1** along the B–Rh axis. Rh is labeled in green, B in orange, P in purple, C in gray and H in black.

The isolation of the rhodium(I) complex **1** from the reaction above mentioned contrasts with the results from similar reactions with Tp ligands, which lead to easy C–H bond activation reactions. As a way of example, the analogous reaction of $[\{Rh(\mu\text{-}Cl)(C_2H_4)_2\}_2]$ with hydrogentris(3,5-dimethylpyrazolyl)borate (Tp^{Me2}) in THF at 0 ºC gives mainly the bis(ethylene)rhodium(I) compound $[(Tp^{Me2})Rh(C_2H_4)_2]$, which renders the butadiene complex $[Rh(Tp^{Me2})(\eta^4\text{-}C_4H_6)]$ on warming.[22] Moreover, addition of acetonitrile to $[(Tp^{Me2})Rh(C_2H_4)_2]$ promotes the formation of the vinylethylrhodium(III) complex $[(Tp^{Me2})Rh(C_2H_3)(C_2H_5)(NCMe)]$.[23] However, no C–H bond activation reactions were detected in our case. Thus, the reaction carried out in d_8-THF gave red-brown solutions containing mainly the highly oxygen-sensitive complex $[(PhBP_3)Rh(CH_2{=}CH_2)(d_8\text{-}THF)]$, which was could not be isolated. However, the two ethylene signals at δ 2.86 and 1.38 ppm observed in the ^1H

NMR spectrum and the two resonances [at δ 55.7 (dt, $J_{Rh,P}$ = 134, $J_{P,P}$ = 25 Hz, 1P, P^M) and 1.04 (dd, $J_{Rh,P}$ =111, $J_{P,P}$ = 25 Hz, 2P, P^A)] in the $^{31}P\{^1H\}$ NMR spectrum support the proposed formulation as the THF equivalent of **1**. Moreover, warming **1** in C_6D_6 lead to a slight broadening of the NMR signals and further to the decomposition of the sample if warming was continued for prolonged times.

Redox behavior of complex 1. Cyclic voltammetry of the complex in acetonitrile at a scan rate of 200 mV/seg showed an irreversible oxidation wave at *ca.* 80 mV versus SCE (Figure 4). On raising the scan rate, a slight increasing of the reversal current intensity was observed, which suggests an EC_{irr} mechanism, *i.e.* an electron transfer reaction followed by an irreversible chemical reaction.

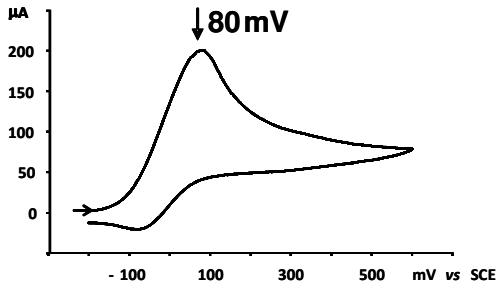

Figure 4. Cyclic voltammogram of complex **1** in acetonitrile (scan rate = 200 mV/seg).

The relatively low value of the oxidation potential makes feasible the chemical oxidation of the complex with a mild oxidant such as $[Cp_2Fe]PF_6$. Monitoring the reaction of **1** with ferrocinium by ^1H and $^{31}P\{^1H\}$ NMR spectroscopy revealed that two molar-equiv of $[Cp_2Fe]PF_6$ were required to consume fully the starting material (**1**), observing no other compounds than the starting material, the product and free ethylene. Hence, the wave in the CV of **1** corresponds to a two-electron oxidation process with release of ethylene. On a preparative scale, the dicationic complex $[(PhBP_3)Rh(NCMe)_3](PF_6)_2$ ($[\mathbf{2}]^{2+}$) was isolated from this reaction as a white crystalline solid in very good yield (Scheme 1).

Scheme 1. Oxidation of $[(PhBP_3)Rh(CH_2{=}CH_2)(NCMe)]$ (**1**) to $[(PhBP_3)Rh(NCMe)_3](PF_6)_2$ ($[\mathbf{2}]^{2+}$).

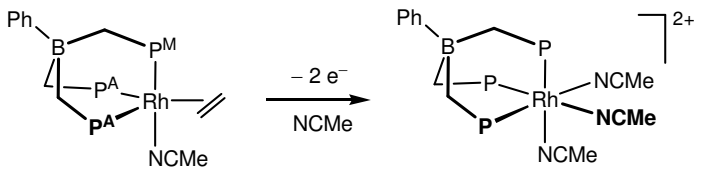

1 $[\mathbf{2}]^{2+}$

Analytical, spectroscopic and structural data of $[\mathbf{2}]^{2+}$ agreed with the proposed formulation (see Experimental Section). Thus, the tree equivalent phosphorus nuclei give a sharp doublet while the three acetonitrile ligands give a singlet (at δ2.29 ppm) in the $^{31}P\{^{1}H\}$ and ^{1}H NMR spectra, respectively. Figure 5 shows the molecular structure of the dication $[\mathbf{2}]^{2+}$ corresponding to the complex $[\mathbf{2}](BF_4)_2$ while selected bond distances and angles are summarized in Table 2.

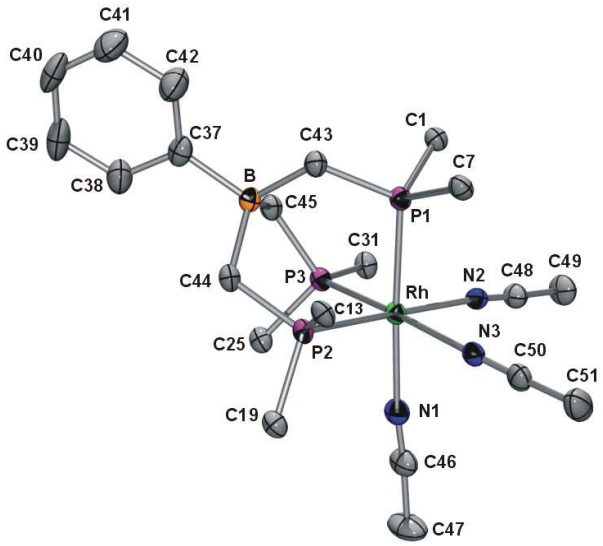

Figure 5. Structure (ORTEP at 50% level) of dicationic complex $[\mathbf{2}]^{2+}$ (hydrogen atoms have been omitted, while only the *ipso* carbons of the phenyl groups are shown for clarity).

Table 2. Selected bond distances (Å) and angles (º) for complex $[\mathbf{2}]^{2+}$.

Rh–P1	2.3392(8)	P1–Rh–P2	86.59(3)
Rh–P2	2.3317(7)	P1–Rh–P3	89.70(3)
Rh–P3	2.3225(8)	P2–Rh–P3	90.50(3)
Rh–N1	2.109(3)	N1–Rh–N2	82.87(9)
Rh–N2	2.112(2)	N1–Rh–N3	84.07(9)
Rh–N3	2.123(3)	N2–Rh–N3	84.84(9)
P1–Rh–N1	176.38(7)	P1–Rh–N2	93.51(6)
P2–Rh–N2	178.48(7)	P1–Rh–N3	95.49(6)
P3–Rh–N3	173.54(6)		

In complex $[(PhBP_3)Rh(NCMe)_3]^{2+}$, the rhodium atom shows the typical octahedral environment of d^6-metal complexes with the tripodal ligand $PhBP_3$ occupying three *fac*-positions while three acetonitrile molecules complete the coordination sphere. Overall, the structure is quite similar to the recently reported ruthenium analogue $[(PhBP_3)Ru(NCMe)_3]^+$.[20] The acetonitrile ligands are squeezed (mean N–Rh–N angle of 83.9 º), presumably as a result of the steric constraints imposed by the phenyl groups on the phosphorus atoms. In addition, the Rh–N bond distances are elongated (averaged value of 2.115 Å), which reflects the steric demands of the $PhBP_3$ ligand and the *trans* influence exerted by members of this class of phosphine ligand.[24]

Reactions of 1 with H_2. The simple exposure of an acetonitrile suspension of complex **1** to hydrogen under atmospheric pressure caused the immediate discoloration of the solution while a white solid separated from the reaction media. This solid was identified as $[(PhBP_3)Rh(H)_2(NCMe)]$ (**3**) by comparison of its spectroscopic data with those of the previously prepared by hydrogenation of $[(PhBP_3)Rh(cod)]$.[19] Although complex **3** is stable in the solid state under argon and in solution in toluene or benzene, leaving these solutions for days produced the crystallization of an orange insoluble solid further identified as the dinuclear complex $[\{(PhBP_3)Rh(H)(\mu\text{-}H)\}_2]$ (**4**) from a X-ray diffraction study. The reaction involves the dissociation of the labile acetonitrile ligand and the dimerisation of the '$(PhBP_3)Rh(H)_2$' fragment through the formation of hydrogen bridges. A similar behavior has been observed for the related iridium complex $[(MeCP_3)Ir(C_2H_4)(H)_2]^+$ ($MeCP_3$ = $MeC(CH_2PPh_2)_3$) which was found to dimerise to the tetrahydride $[\{(MeCP_3)Ir(H)(\mu\text{-}H)\}_2]^{2+}$ with evolution of ethylene on heating the solid.

Figure 6 shows the molecular structure of **4** while Table 3 collects selected bond distances and angles. As anticipated, the X-ray structure of **4** revealed it to be a dinuclear edge-sharing bioctahedral complex with two bridging hydrides and one terminal hydride on each rhodium atom; the two halves of the molecule are related by an inversion center. All hydrides were located[25] in a difference-Fourier map and refined with some geometrical constraints.

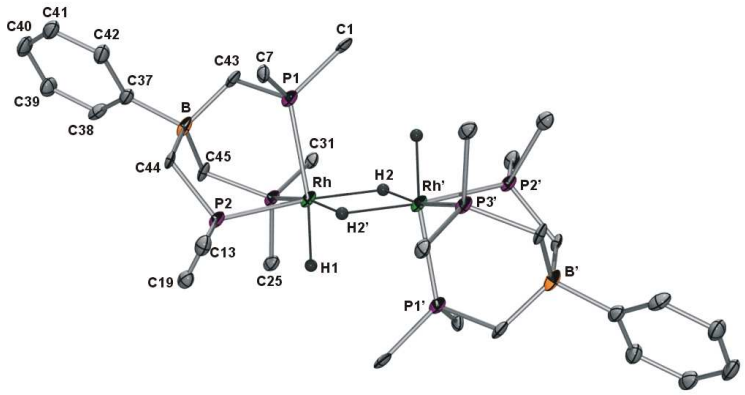

Figure 6. Structure (ORTEP at 50% level) of complex **4** (hydrogen atoms except hydride ligands have been omitted and only the *ipso* carbons of the phenyl groups are shown for clarity).

Table 3. Selected bond distances (Å) and angles (º) for complex **4**.

Rh–P1	2.4252(13)	P1–Rh–P2	90.38(5)
Rh–P2	2.2813(14)	P1–Rh–P3	90.61(5)
Rh–P3	2.2995(13)	P2–Rh–P3	83.97(5)
Rh–H1	1.59	P1-Rh-H1	171.8
Rh–H2	1.87(2)	P2-Rh-H2	174.6(13)
Rh–H2’	1.86(4)	P3-Rh-H2’	170.2(11)

Dinuclear rhodium complexes with the ‘$\{Rh(H)(\mu\text{-}H)\}_2$’ core are quite uncommon, being the dicationic $[\{(C_n)Rh(H)(\mu\text{-}H)\}_2]^{2+}$ (C_n = 1,4,7-trimethyl-1,4,7-triazacyclononane),[26] the single crystallographically characterized precedent found in the Cambridge Structural Database. Nonetheless, complexes of the type $[\{(MeCP_3)Rh(H)(\mu\text{-}H)\}_2]^{n+}$ (n = 2, 1, 0; $MeCP_3$ = $MeC(CH_2PPh_2)_3$) have been previously reported by Bianchini.[27] The rhodium–rhodium distance in **4** (2.8152(9)Å) was found to be longer than in $[\{(C_n)Rh(H)(\mu\text{-}H)\}_2]^{2+}$ (2.595(2) Å) probably due to the steric overcrowding generated by the phenyl groups in $PhBP_3$. In fact, metal–metal distances for related iridium complexes having ‘$\{Ir(H)(\mu\text{-}H)\}_2$’ cores lie in the range 2.79-2.70.[28]

Complex **4** has a 32 valence-electron (v.e.) count, so that for satisfying the 18-electron rule a formal rhodium–rhodium double bond would be required. However, under the perspective of two formally

electron-deficient 16 v.e. centers it is not necessary to postulate a metal–metal bond; the best description of the bonding between the two halves of the complex corresponds to two delocalized 3c-2e M–H–M bonds, as proposed by Braunstein for the complex $[\{(N_2P)Ir(H)(\mu\text{-}H)\}_2]^{2+}$ (N_2P = bis(oxazoline)phosphonite).[28b]

Furthermore**,** exposure of the dihydride complex **3** to an oxygen atmosphere gives an orange solid identified as the dioxygen compound $[\{(PhBP_3)Rh(\mu\text{-}O_2)\}_2]$.[6] The reaction was found to be fully reversible, and $[\{(PhBP_3)Rh(\mu\text{-}O_2)\}_2]$ transforms into $[(PhBP_3)Rh(H)_2(NCMe)]$ (**3**) by reaction with hydrogen in acetonitrile.

Initial experiments on the reaction of **1** with hydrogen in tetrahydrofuran were disappointing because a red product could be isolated in variable yields depending apparently on the reaction conditions. Once isolated, the red complex was identified as the paramagnetic hydride $[\{(PhBP_3)Rh\}_2(\mu\text{-}H)_3]$ (**5**) (see below), which showed broad signals in the ^1H NMR and flat $^{31}P\{^1H\}$ NMR spectra. Nonetheless, monitoring the reaction of **1** with hydrogen in d_8-THF showed a clean formation of the diamagnetic complex $[(PhBP_3)Rh(H)_2(NCMe)]$ (**3**), which did not give **5** when air was allowed to enter in the NMR tube. After discarding that traces of oxygen were the responsible for this reaction, the radical trap TEMPO (2,2,6,6-tetramethylpiperidin-1-yl)oxyl) was tested as hydrogen abstractor although without success. Finally, transformation of complex **3** into **5** was achieved in the presence of 3,5-dimethyl-4-hydroxytoluene, similar to 3,5-di-*tert*-butyl-4-hydroxytoluene (BHT), the usual stabilizing agent for THF. Therefore, complex **5** resulted from the reaction of **3** with BHT contained in the solvent. Figure 7 shows the molecular structure of **5** while selected bond distances and angles are collected in Table 4.

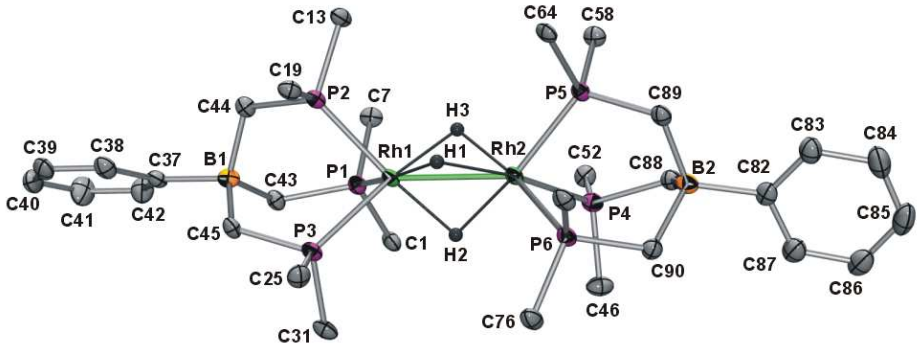

Figure 7. Structure (ORTEP at 50% level) of complex **5** (hydrogen atoms except hydride ligands have been omitted, and only the *ipso* carbons of the phenyl groups are shown for clarity).

Complex **5** is formed by two '$(PhBP_3)Rh$' subunits bridged by three hydrogen atoms. The geometry around each rhodium atom is almost octahedral, with angles close to 90º (see Table 4).

According to the neutral nature of the complex, it is a mixed-valence Rh(II)/Rh(III) compound with an electron count of 31 v.e., i.e. one electron less than the tetrahydride complex **4** in which there is not a metal–metal bond. Apart from the delocalized 3c-2e bonds, the electron counting rules require in this case to propose a metal-metal bond with a Rh–Rh bond order of 0.5 for **5.** Accordingly, a relatively short rhodium–rhodium bond distance (2.6488(6) Å) is observed. This distance is quite similar to that found in the Rh(II)/Rh(III) dicationic complex $[\{(MeCP_3)Rh\}_2(\mu\text{-}H)_3]^{2+}$ (2.644(1) Å),[29] and, as expected, longer that those found in the related 30 v.e. Ir(II)/Ir(II) complex $[\{(Cp^*)Ir\}_2(\mu\text{-}H)_3]^{+}$ having a single iridium–iridium bond (averaged metal-metal bond distances are 2.47 Å).[30]

Table 4. Selected bond distances (Å) and angles (º) for complex **5**.

Rh1–P1	2.3410(10)	Rh2–P4	2.3682(10)
Rh1–P2	2.3073(11)	Rh2–P5	2.3080(9)
Rh1–P3	2.3347(10)	Rh2–P6	2.3137(10)
Rh1–H1	1.87(4)	Rh2–H1	1.91(4)
Rh1–H2	1.82(4)	Rh2–H2	1.86(3)
Rh1–H3	1.83(3)	Rh2–H3	1.92(3)
P1–Rh1–P2	89.76(3)	P4–Rh2–P5	87.18(4)

P1–Rh1–P3	89.58(3)	P4–Rh2–P6	91.10(4)
P2–Rh1–P3	86.83(3)	P5–Rh2–P6	85.73(3)
P1-Rh1-H1	165.9(11)	P4-Rh2-H1	168.7(11)
P2-Rh1-H2	170.0(11)	P5-Rh2-H2	173.3(11)
P3-Rh1-H3	173.3(12)	P6-Rh2-H3	167.5(10)

Reactions of complexes 1 and 3 with electrophiles. Addition of one mol-equiv. of HBF_4 to an acetonitrile suspension of **1** gave clean and quantitatively the cationic hydride complex $[(PhBP_3)Rh(H)(NCMe)_2]BF_4$ ($[\mathbf{6}]^+$), which was isolated as a pale-yellow solid (Scheme 2). Spectroscopic data of $[\mathbf{6}]^+$ agree with the proposed structure. Thus, the hydride resonance was located at δ –7.09 ppm in the ^{1}H NMR spectrum as a doublet of pseudoquartets [$J_{H,PA}$ = 187.2 Hz, $J_{H,PM}$ = 7.8 Hz and $J_{H,Rh}$ = 7.8 Hz], while the ν(Rh–H) stretching was found at 1989 cm^{-1} in the IR spectrum. The inequivalent phosphorus nuclei produce two signals in a 2:1 ratio [at δ 43.8 (dd, P^M) and 1.3 (dt, P^A) ppm] in the $^{31}P\{^1H\}$ NMR spectrum, corresponding to an AM_2X spin system (X = ^{103}Rh). According to its ionic nature, complex $[\mathbf{6}]BF_4$ behaves as a 1:1 electrolyte in acetone solutions. The reaction was found to be fully reversible, and thus, complex $[\mathbf{6}]^+$ regenerates **1** upon saturation of the acetonitrile solution with ethylene and addition of one molar-equiv. of KOH (^{1}H NMR evidence) (Scheme 2).

Scheme 2. Relationships between complexes **1**, **3**, $[\mathbf{2}]^{2+}$ and $[\mathbf{6}]^+$

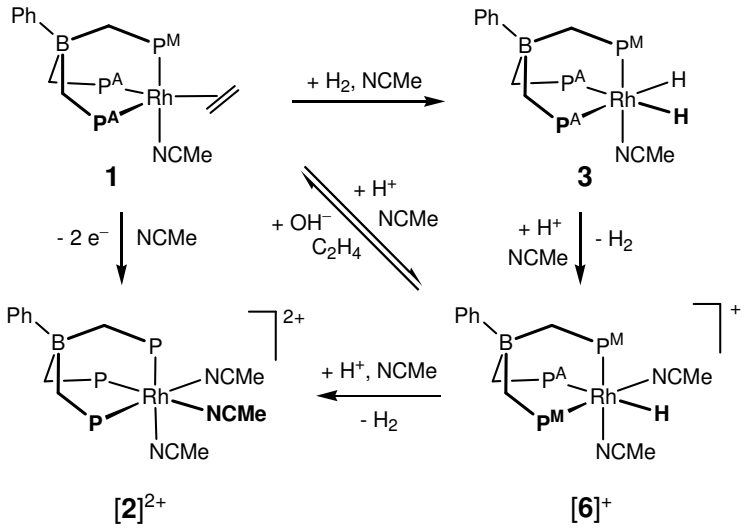

Complex $[\mathbf{6}]^+$ also results from the protonation of the dihydride $[(PhBP_3)Rh(H)_2(NCMe)]$ (**3**) with HBF_4 in the presence of acetonitrile. Moreover, addition of two molar-equiv. of HBF_4 to solutions of **3** in C_6D_6 caused the slow crystallization of a white crystalline solid characterized as $[(PhBP_3)Rh(NCMe)_3](BF_4)_2$ ($[\mathbf{2}]^{2+}$, along with hydrogen release (Scheme 2).[31] As expected, a further addition of one molar-equiv. of HBF_4 and acetonitrile to CD_2Cl_2 solutions of $[\mathbf{6}]^+$ gave rise to the clean formation of $[\mathbf{2}]^{2+}$ along with hydrogen evolution.[31]

Hydride protonation reactions have been extensively used for the preparation of dihydrogen complexes of the type $[L_nM(\eta^2\text{-}H_2]$, mainly for complexes of group 8 transition metals.[32] However, such type of complex was not isolated in our case, and H_2 elimination with coordination of acetonitrile seems to be the driving force for the protonation reaction. Overall, the sequence $\mathbf{1} \rightarrow [\mathbf{6}]^+ \rightarrow [\mathbf{2}]^{2+}$ constitutes an example for the reduction of 2 H^+ to H_2 promoted by a rhodium compound, which provides the two required electrons.

Quite different results were obtained when complex **1** was protonated with acids having a coordinating anion, such as benzoic or acetic. The kinetic products were found to be the ethyl complexes $[(PhBP_3)Rh(\eta^1\text{-}C_2H_5)(\kappa^2\text{-}O_2CR)]$ (R = Ph, **7**; Me, **8**), which establish an equilibrium in solution with the corresponding hydride complexes $[(PhBP_3)Rh(H)(\kappa^2\text{-}O_2CR)]$ (R = Ph, **9**; Me, **10**) and free ethylene (Scheme 3). In both cases, once the thermodynamic equilibria were reached, ^{1}H NMR spectra showed a 45:55 ratio (**7**:**9**) and 30:70 for (**8**:**10**). Accordingly, pure samples of **7** and **8** were obtained by carrying out the reactions under an atmosphere of ethylene.

Scheme 3. Reactions of **1** and **3** with carboxylic acids.

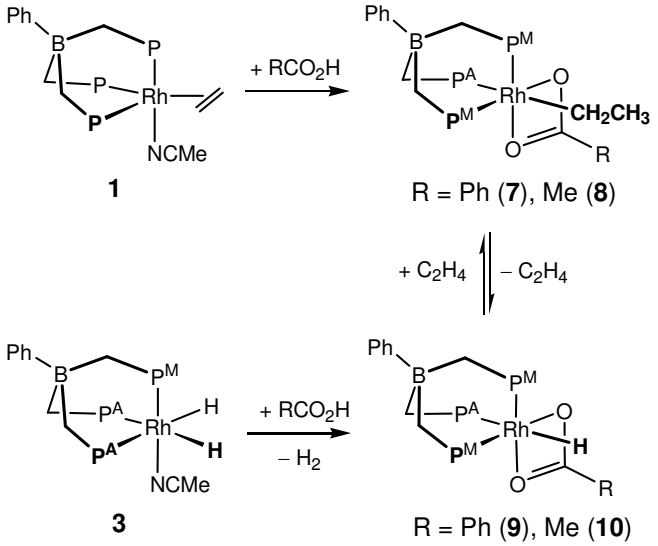

1 R = Ph (**7**), Me (**8**)

3 R = Ph (**9**), Me (**10**)

The ethyl group in **7** and **8** was clearly identified in the $^{1}H\{^{31}P\}$ NMR spectra from the sharp quartet and triplet at chemical shifts of *ca.* δ 1.53 and 0.87 ppm, respectively. The carbon signal from the coordinated carboxylate ligand was localized from $^{1}H,^{13}C$-hmbc experiments at δ 179.9 and 185.9 ppm, respectively. The $^{31}P\{^{1}H\}$ NMR spectra show the typical pattern for an AM_2X spin system, according to the C_s symmetry of the complexes with the carboxylate as chelating ligand. The phosphorus *trans* to the ethyl group (P^A) resonates, in both cases, at high field (δ 2.9 and 3.4 ppm, respectively) and it is noticeable the low value for the $J_{P,Rh}$ for this signal (around 66 Hz) when compared to those for the phosphorous *trans* to the acetate ligands (P^M, around 130 Hz). The related hydride derivatives **9** and **10** were cleanly prepared from the reactions of the dihydride complex **3** with the corresponding acids. Analytical and spectroscopic data for both agree with the proposed formulation (see Experimental Section).

Formation of the ethyl-derivatives $[(PhBP_3)Rh(\eta^1\text{-}C_2H_5)(\kappa^2\text{-}O_2CR)]$ (R = Ph, **7**; Me, **8**) requires some comments. Starting from **1**, a first step in which the acetonitrile ligand is replaced by the carboxylic acid to form adducts of the type **A** (Scheme 4) can be assumed. At this point, two paths can be proposed for the next step of the reaction. Path i) involves protonation at the rhodium(I) center by the acidic HO_2C–proton (to give **B**) followed by a β-migratory insertion to give the ethyl-intermediate **C** and coordination of the second oxygen atom from the carboxylate to result in the complexes **7**-**8**. Alternatively, path ii)

would start with the direct attack of the proton to the coordinated ethylene to produce the ethyl-complex **C** followed by coordination of the free oxygen atom. This picture has been suggested in some instances.[33] However, the most common accepted way for the reactions of complexes of late transition metals with acids is the protonation of the metal to give hydride derivatives,[34] and in less extension, to an heteroatom bonded to the metal if it contains free electron pairs, for example an acac ligand.[35] In our case, this third possibility would produce the rhodium(I) intermediate [(PhBP$_2$PH)Rh(C$_2$H$_4$)(κ^1-O$_2$CR)], as may occur in the reaction of **1** with the electrophile Me$^+$ to which ethylene evolution follows (see below). However, this sequence with the electrophile H$^+$ would result in the product [(PhBP$_2$PH)Rh(κ^2-O$_2$CR)], which is not the case, since the products of the reaction are complexes **7**-**10**. Nonetheless, which site is protonated firstly: metal (path i) or carbon (path ii) is a difficult question to answer.[36] We believe that protonation at the carbon is the most probable event (path ii), since the high electronic density at the ethylene coming from the strong π-back donation.

Scheme 4. Alternative paths for the synthesis of complexes **7**-**10**.

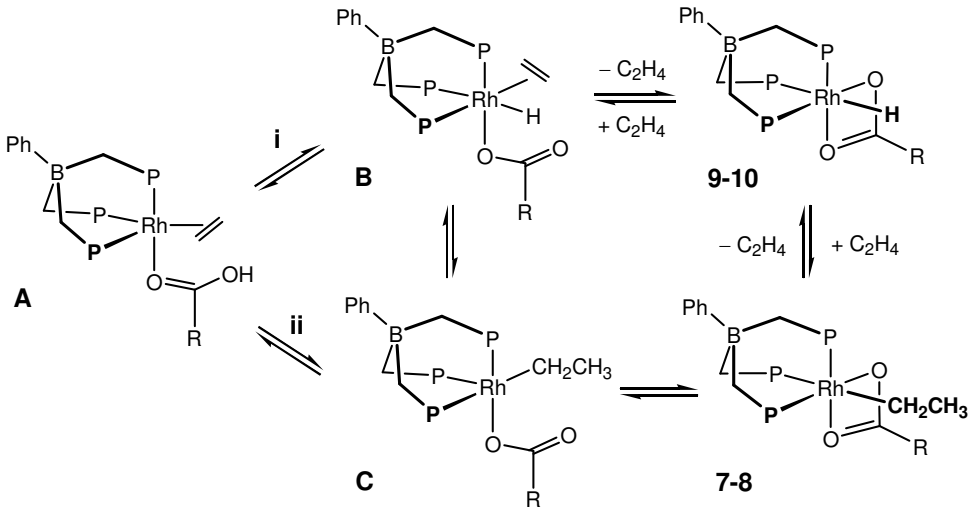

Starting from the ethyl-complexes (**7**-**8**), a *β*-elimination reaction to the hydride ethylene complex **B** (through the intermediate C) provides an easy way for ethylene evolution and formation of the hydride complexes **9**-**10**. In the reverse sense, starting from the hydride derivatives [(PhBP$_3$)Rh(H)(κ^2-O$_2$CR)]

(R = Ph, **9**; Me, **10**), the thermodynamic equilibria are again established on dissolved the complexes in C_6D_6 saturated with ethylene. This reversibility seems to suggest that the hydride-ethylene (**B**, Scheme 4) is a key common intermediate.

Other electrophiles such as Me^+ were also tested as suitable for C–C and/or P–C bond formation reactions. In this sense, complex **1** reacted almost immediately with MeOTf to give the complex alkylated at the phosphorus atom (P–methyl) [{PhB(PMe)P_2}Rh(κ^2-O_2SOCF_3)] (**11**) (Scheme 5). Spectroscopic and analytical data of **11** agree with the proposed formulation (see Experimental Section). Thus, the most relevant spectroscopic data are two resonances in the $^{31}P\{^1H\}$ NMR spectrum; the doublet corresponds to two phosphorus nuclei bound to rhodium while the singlet at low field (δ 74.8 ppm) is due to the quaternization of the third phosphorus atom. Accordingly, the signals of the $-CH_2$ and $-CH_3$ groups bonded to this atom (P^M) are also low-field shifted at δ 4.06 ($J_{H,P}$ = 12.4 Hz) and 2.81 ($J_{H,P}$ = 12.9 Hz) ppm, respectively, in the ^1H NMR spectrum.

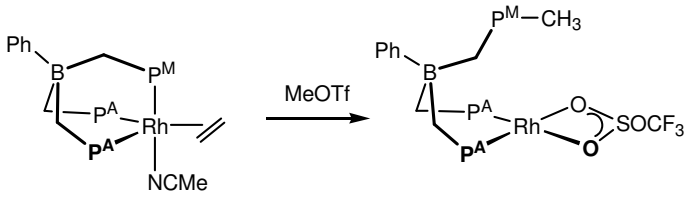

1 **11**

Scheme 5. Synthesis of complex **11** containing an alkylated phosphorus atom.

Finally, it should be indicated that chloride should be avoided in the reactions involving the above mentioned cationic complexes, since it replaces very easily the labile acetonitrile ligands. As a way of example, the cationic complex [($PhBP_3$)Rh(H)($NCMe)_2$]BF_4 ([**6**]$^+$) transforms into the neutral [{($PhBP_3$)Rh(H)(μ-Cl}$_2$][19] by reaction with PPNCl (PPN = bis(triphenylphosphoranylidene)ammonium), while the dicationic [($PhBP_3$)Rh($NCMe)_3$]$^{2+}$ ([**2**]$^{2+}$) gave the dinuclear triple bridged complex [{($PhBP_3$)Rh}$_2$(μ-Cl)$_3$]$^+$ ([**12**]$^+$) in the presence of PNNCl and eventually [($PhBP_3$)Rh($Cl)_2$]. Complex [**12**]$^+$ was also obtained by reacting [($PhBP_3$)Rh($Cl)_2$][19] with 0.5

molar-equiv. of methyl triflate (MeOTf) in a reaction in which one chloride ligand is eliminated as MeCl (Scheme 6) (see Experimental Section). Notice that the use of MeOTf to abstract terminal halide ligands represents a clean reaction that usually renders halide-bridged complexes,[37] as an alternative to the use of silver salts.

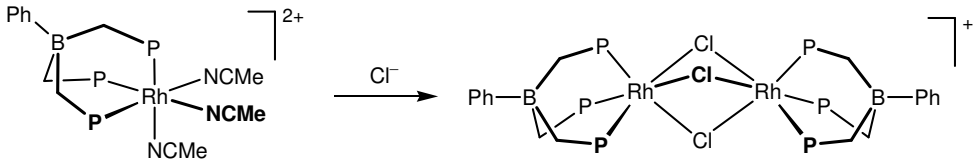

[**2**]$^{2+}$ [**12**]$^{+}$

Scheme 6. Synthesis of complex [**12**]$^{+}$.

According to the C_3 symmetry of complex [**12**]$^{+}$, a sharp doublet at δ 33.5 ppm was found in the $^{31}P\{^{1}H\}$ NMR spectrum. In addition, the nuclearity of the complex has been confirmed from the measurement of the coefficient of diffusion by NMR methods. Thus, DOSY experiments on [**12**]$^{+}$ gave a value of D = 4.37 10^{-10} m^2/s, similar to that reported for the related dinuclear complexes [{$(PhBP_3)Rh(\mu\text{-}O_2)$}$_2$] and [{$(PhBP_3)Rh$}$_2(\mu\text{-}O_2)(\mu\text{-}OOH)]^{+}$, and quite lower than that observed for mononuclear complexes.[6] Finally, preliminary X-ray diffraction studies on a crystal of low-quality (see Supporting Information) confirmed the proposed structure, being similar to that reported for the tricationic complexes of the type [{$(MeCP_3)Rh$}$_2(\mu\text{-}Cl)_3]^{3+}$.[38]

Summary and conclusions

In summary, we have shown that a chemistry based on the '$(PhBP_3)Rh$' scaffold is easily accessible through the rhodium(I) complex [$(PhBP_3)Rh(CH_2{=}CH_2)(NCMe)$] (**1**) with labile ligands ethylene and acetonitrile. Reactivity studies on **1** have revealed it to be a very reactive species, easily oxidized by chemical oxidants and suitable for a fast reaction with hydrogen, affording the rhodium(III) complexes $[(PhBP_3)Rh(NCMe)_3]^{2+}$ ([**2**]$^{2+}$) and $[(PhBP_3)Rh(H)_2(NCMe)]$ (**3**), respectively. The neutral dihydride complex **3** was found to be stable in solution, but undergoes slow dissociation of acetonitrile and

dimerises through the formation of hydrogen bridges to [{(PhBP$_3$)Rh(H)(μ-H)}$_2$] (**4**). Complex **3** can be also prepared in other solvents such as THF if free of stabilizing agents like BHT. Otherwise, hydrogen abstraction to the red paramagnetic complex [{(PhBP$_3$)Rh}$_2$(μ-H)$_3$] (**5**) takes place. Hydride ligands in **3** possess a basic character and they are sequentially protonated (and removed as hydrogen) to eventually form [**2**]$^{2+}$ through the cationic monohydride intermediate [(PhBP$_3$)Rh(H)(NCMe)$_2$]$^+$ ([**6**]$^+$). The overall sequence **1** → [**6**]$^+$ → [**2**]$^{2+}$ constitutes an example for the reduction of 2 H$^+$ to H$_2$ promoted by a rhodium compound, which provides the required electrons. On the other hand, the nucleophilic nature of complex **1** has been demonstrated from its reactions with several Brönsted acids. Protonation of **1** with HBF$_4$ in acetonitrile is accomplished by ethylene evolution and formation of the monohydride [**6**]$^+$. Similar reactions with carboxylic acids, such as benzoic or acetic, retain the ethylene ligand as an ethyl group in complexes of the type [(PhBP$_3$)Rh(η^1-C$_2$H$_5$)(κ^2-O$_2$CR)] (**7**-**8**). Most probably these reactions occur by a direct attack of the nucleophile H$^+$ at the coordinated ethylene in **1**, due to the high electronic density at the ethylene coming from the strong π-back donation. The ethyl complexes **7**-**8** establish an equilibrium with the corresponding hydride compounds [(PhBP$_3$)Rh(H)(κ^2-O$_2$CR)] (**9**-**10**) with ethylene loss. Both type of complexes are related by a *β*-hydrogen elimination (from **7**-**8** to **9**-**10**) and hydride insertion in the opposite way, requiring the non observed hydride complex [(PhBP$_3$)Rh(H)(C$_2$H$_4$)(κ^1-O$_2$CR)] as a common intermediate. In other instances, P–C bond formation reactions take place as revealed in the reactions of complex **1** with methyltriflate to give [{PhB(PMe)P$_2$}Rh(κ^2-O$_2$SOCF$_3$)]. Further studies to develop the potential of the '(PhBP$_3$)Rh' scaffold in stoichiometric and catalytic reactions are currently in progress.

Experimental Section.

Starting Materials and Physical Methods. All the operations were carried out under an argon atmosphere using standard Schlenk techniques. Solvents were dried and distilled under argon before use

by standard methods.[39] Complexes [{Rh(μ-Cl)(C_2H_4)}$_2$],[40] [($PhBP_3$)Rh($Cl)_2$],[19] and [Li(tmen)][PhB($CH_2PPh_2)_3$][8] were prepared according to literature methods. Other reagents were commercially available and were used as received. Elemental analyses were performed using a Perkin-Elmer 2400 microanalyzer. FAB^+ mass spectra were recorded in a VG Autospec double-focusing mass spectrometer and 3-nitrobenzyl alcohol (NBA) was used as matrix. MALDI-TOF^+ mass spectra were obtained on a Bruker Microflex mass spectrometer using DCTB (*trans*-2-[3-(4-*tert*-butylphenyl)-2-methyl-2-propenylidene]malononitrile) as matrix. NMR spectra were recorded on Bruker AV 300 and AV 400 spectrometers operating at 300.13 and 400.13 MHz, respectively, for ^1H. Chemical shifts are reported in ppm and referenced to $SiMe_4$, using the internal signal of the deuterated solvent as reference (^1H, ^{13}C) and external H_3PO_4 (^{31}P). IR spectra in solution were recorded with a Nicolet 550 spectrophotometer using NaCl cells, while IR spectra of solid samples were recorded with a Perkin-Elmer 100 FT-IR Spectrometer (4000-400 cm^{-1}) equipped with an ATR (Attenuated Total Reflectance). Conductivities were measured in acetone solutions using a Philips PW 9501/01 conductimeter. Electrochemical experiments were performed by means of an EG&G Research Model 273 potentiostat/galvanostat. A three-electrode glass cell consisting of a platinum-disk working electrode, a platinum-wire auxiliary electrode and a KCl saturated calomel reference (SCE) electrode was employed. Linear voltamperometry was performed by using a rotating platinum electrode (RDE) as the working electrode. The supporting electrolyte solution (NBu_4PF_6, 0.1 M) was scanned over the solvent window to ensure the absence of electroactive impurities curves. A concentration of complex **1** of about 5 10^{-4} M was employed in all the measurements.

Synthesis of the Complexes: [($PhBP_3$)Rh(CH_2=CH_2)(NCMe)] (1). A Schlenk tube was charged with solid [{Rh(μ-Cl)($C_2H_4)_2$}$_2$] (120.0 mg, 0.31 mmol) and solid [Li(tmen)][PhB($CH_2PPh_2)_3$] (499.0 mg, 0.62 mmol). Addition of deoxygenated acetonitrile (3 mL) produced the dissolution of the starting materials while an orange crystalline solid precipitated almost immediately. After stirring for 20 min, the solid was separated by decantation, washed with cold acetonitrile (3 x 3 mL) and vacuum-dried. In this way complex **1** crystallizes with two molecules of acetonitrile. Yield: 471.9 mg (81 %). ^1H NMR (400

MHz, CD_2Cl_2, −50 ºC): δ 8.29 (br s, 2H, BPh^o), 7.70-6.60 (33H, Ph), 2.48 (d, J = 6.6 Hz, 2H, CH_2=CH_2), 1.65 (δ_A, 2H) and 1.14 (δ_B, 2H, J_{AB} = 14.3 Hz, CH_2P^A), 1.48 (br, 2H, CH_2=CH_2), 1.38 (s, 3H, $NCCH_3$), 1.15 (br, 2H, CH_2P^M). $^{31}P\{^1H\}$ NMR (162 MHz, CD_2Cl_2, −50 ºC): δ 43.8 (dt, $J_{P,Rh}$ = 124, $J_{P,P}$ = 34 Hz, 1P, P^M), 12.5 (dd, $J_{P,Rh}$ = 110, $J_{P,P}$ = 34 Hz, 2P, P^A). $^{13}C\{^1H\}$ NMR (100 MHz, CD_2Cl_2, −50 ºC) from ^1H,^{13}C-hsqc and ^1H,^{13}C-hmbc spectra: δ 119.3 (N*C*CH_3), 34.1 (CH_2=CH_2), 16.7 (CH_2P^M), 13.4 (CH_2P^A), 2.8 (NC*C*H_3). MS (FAB^+): *m/z* (%): 788 (100) $[(PhBP_3)Rh]^+$. Anal. Calcd (%) for $C_{49}H_{48}NBP_3Rh\cdot 2(NCCH_3)$ (939.68): C 67.74, H 5.79, N 4.47; found: C 67.97, H 5.65, N 4.42.

$[(PhBP_3)Rh(NCMe)_3](PF_6)_2$ ($[2]^{2+}$). To a solution of **1** (66.7 mg, 0.071 mmol) in dichloromethane/acetonitrile (4/0.5 mL), $[Fe(C_5H_5)_2]PF_6$ (47.1 mg, 0.142 mmol) was added. The mixture was stirred for 1 h and then evaporated to dryness. The residue was washed with diethyl ether (3 x 5 mL) in order to remove $[Fe(C_5H_5)_2]$ and then dissolved dichloromethane (2 mL) and carefully layered with diethyl ether (10 mL). The white crystalline solid deposited in three days was separated by decantation, washed with cold diethyl ether and vacuum-dried. Yield: 72.8 mg (85 %).

Alternatively, complex $[(PhBP_3)Rh(NCMe)_3](BF_4)_2$ can be prepared from the addition of $HBF_4\cdot Et_2O$ (12.0 μL, 0.086 mmol) and acetonitrile (4.5 μL, 0.086 mmol) to a dichloromethane solution of **1** (40.4 mg, 0.043 mmol in 3 mL). The white microcrystals deposited in two days were separated by decantation, washed with hexane (2 x 3 mL) and vacuum-dried. . Yield: 47.6 mg (93 %). ^1H NMR (300 MHz, CD_2Cl_2, 25 ºC): δ 7.59 (d, J = 7.1 Hz, 2H, BPh^o), 7.47 (t, $J_{H,P}$ = 7.2 Hz, J = 7.1 Hz, 18H, $Ph_2{}^{o+p}P$), 7.38 (t, J = 7.2 Hz, 2H, BPh^m), 7.31 (t, J = 7.4 Hz, 12H, $Ph_2{}^mP$), 7.22 (t, J = 7.3 Hz, 1H, BPh^p), 2.29 (s, 9H, $NCCH_3$), 1.77 (br d, $J_{H,P}$ = 8.6 Hz, 6H, CH_2P). $^{31}P\{^1H\}$ NMR (121 MHz, CD_2Cl_2, 25 ºC): δ 32.3 (d, $J_{P,Rh}$ = 103 Hz, 3P), −144.2 (sept, $J_{P,F}$ = 711 Hz, 1P, PF_6^-). MS (MALDI-TOF^+): *m/z* (%): 788 (66) $[(PhBP_3)Rh]^+$. Anal. Calcd (%) for $C_{51}H_{50}BF_{12}N_3P_5Rh$ (1201.53): C 50.98, H 4.19, N 3.50; found: C 50.57, H 4.26, N 3.53. Λ_M (5.0 x 10^{-4} in acetone) = 129.5 S mol^{-1} cm^{-1}.

$[(PhBP_3)Rh(H)_2(NCMe)]$ (3). Exposure of solutions of **1** in acetonitrile/toluene (1:5) to an atmosphere of hydrogen causes an immediate discoloration. ^1H NMR of an aliquot indicated the

quantitative transformation of **1** into the dihydride complex **3** previously reported.[19] From these solutions, complex **3** was isolated after concentration of the solution and precipitation with hexane. Isolated yield: 80%.

Reaction of 1 with H_2 in d_8-THF**.** A NMR-tube was charged with complex **1** (10.3 mg, 0.011 mmol) and then dissolved in deoxygenated and free of BHT d_8-THF (0.5 mL)**.** Exposure of the solution to hydrogen for 5 min caused discoloration of the solution and the clean formation of **3** was observed. Selected spectroscopic data: ^{1}H NMR (300 MHz, d_8-THF, 25 ºC): δ 7.77 (t, $J_{H,P}$ = 7.9 Hz, J = 7.9 Hz, 4H, $Ph_2{}^{o1}P^A$), 7,73 (ddd, $J_{H,P}$ = 11.5 Hz, J = 8.9 Hz, J = 1.7 Hz, 4H, $Ph_2{}^{o}P^M$), 7,56 (d, J = 7.4 Hz, 2H, BPh^{o}), 7.15 (J = 7.4 Hz, 2H, BPh^{m}), 7.05 (m, 12H, $Ph_2{}^{o2+m2+p2}P^A$, $Ph_2{}^{p}P^M$), 6.96 (t, J = 6.9 Hz, 4H, $Ph_2{}^{m1}P^A$), 6.94 (td, J = 8.5 Hz, J = 1.7 Hz, 6H, $Ph_2{}^{m}P^M$ + $Ph_2{}^{p1}P^A$), 6.77 (t, J = 7.5 Hz, 1H, BPh^{p}), 1.64 (s, 3H, $NCCH_3$), 1.71 (δ_A, 2H) and 1.30 (δ_B, 2H, J_{AB} = 12 Hz, CH_2P^A), 1.20 (d, $J_{H,P}$ = 13.7 Hz, 2H, CH_2P^M), –7.66 (ddd, $J_{H,PA}$ = 158.3 Hz, $J_{H,PM}$ = 9.7 Hz, $J_{H,Rh}$ = 14.2 Hz, 1H, Rh–H). ^{31}P{^{1}H} NMR (121 MHz, d_8-THF, 25 ºC) δ 53.7 (dt, $J_{P,Rh}$ = 130 Hz, $J_{P,P}$ = 28 Hz, 1P, P^M), 22.4 (dd, $J_{P,Rh}$ = 79 Hz, $J_{P,P}$ = 28 Hz, 2P, P^A). ^{13}C{^{1}H} NMR (100 MHz, d_8-THF, 25 ºC) from ^{1}H,^{13}C-hsqc and ^{1}H,^{13}C-hmbc spectra: δ 119.8 ($NCCH_3$), 16.2 (CH_2P^A), 15.7 (CH_2P^M), 1.18 ($NCCH_3$).

[{(PhBP$_3$)Rh(H)(μ-H)}$_2$] (4). A solution of [(PhBP$_3$)Rh(H)$_2$(NCMe)] (**3**) (15.0 mg, 0.018 mmol) in C_6D_6 (0.5 mL) was maintained undisturbed under an atmosphere of hydrogen. Orange microcrystals were deposited on a week. The crystals were separated by decantation, washed with pentane (2 x 2 mL) and vacuum-dried. Yield: 10.7 mg (75 %). IR (solid): ν(Rh–H)/cm^{-1}: 2007 (m). Anal. Calcd (%) for $C_{90}H_{86}B_2P_6Rh_2$ (1580.92): C 68.38, H 5.48; found: C 68.49, H 5.63.

[{(PhBP$_3$)Rh}$_2$(μ-H)$_3$] (5). A solution of **1** (56.4 mg, 0.060 mmol) in tetrahydrofuran (3 mL) that contained traces of BHT was kept under an atmosphere of hydrogen overnight, developing a red color. The reaction was monitored by ^{1}H NMR, while additional volumes of THF were added to drive the reaction to completion in two days. The resulting red solution was evaporated to dryness and the residue was dissolved in toluene (3 mL), filtered through celite and carefully layered with hexane (10 mL). The red crystalline solid deposited in three days was separated by decantation, washed with hexane (2 x 3

mL) and vacuum-dried. Yield: 33.2 mg (70 %). IR (CH_2Cl_2): ν(Rh–H)/cm^{-1}: 1636 (m). ^{1}H NMR (300 MHz, C_6D_6, 25 ºC): δ 11.57 (br s), 8.34-6.33 (br), 7.56 (d, J = 7.1 Hz, 2H, BPh^{o}), 7.37 (t, J = 7.1 Hz, 2H, BPh^{m}), 7.28 (t, J = 7.1 Hz, 1H, BPh^{p}), 3.69 (br), 1.72 (br). MS (MALDI-TOF$^+$): *m/z* (%): 1579 (100) [M]$^+$, 789 (81) [(PhBP$_3$)Rh(H)]$^+$. Anal. Calcd (%) for $C_{90}H_{85}B_2P_6Rh_2$ (1579.92): C 68.42, H 5.42; found: C 68.16, H 5.20.

[(PhBP$_3$)Rh(H)(NCMe)$_2$]BF$_4$ ([6]$^+$). $HBF_4{\cdot}Et_2O$ (11.7 μL, 0.085 mmol) and acetonitrile (10.0 μL, 0.192 mmol) were added to a solution of **1** (80.0 mg, 0.085 mmol) in dichloromethane (4 mL) at −50 ºC. The resulting yellow solution was allowed to reach room temperature and then it was concentrated to *ca.* 2 mL and carefully layered with hexane (8 mL) to give a yellow solid. The product was filtered off, washed with hexane (2 x 5 mL) and vacuum-dried. Yield: 61.1 mg (75 %). IR (CH_2Cl_2): ν(Rh–H)/cm^{-1}: 1989 (m), ν(N≡C)/cm^{-1}: 2304 (m). ^{1}H NMR (400 MHz, CD_2Cl_2, 25 ºC): δ 7.65 (m, 6H, Ph$_2{}^{o1}$P^M + BPh^{o}), 7.56 (t, J = 8.6 Hz, 4H, Ph$_2{}^{o}$P^A), 7.35 (m, 9H, Ph$_2{}^{m}$P^A + Ph$_2{}^{p1}$P^M + BPh^{m+p}), 7.22 (m, 4H, Ph$_2{}^{m2}$P^M), 7.07 (m, 12H, Ph$_2{}^{o2}$P^M + Ph$_2{}^{m1}$P^M + Ph$_2{}^{p}$P^A + Ph$_2{}^{p2}$P^M), 2.01 (s, 6H, NCCH$_3$), 1.72 (d, $J_{H,P}$ = 11.7 Hz, 2H, CH$_2$P^A), 1.56 (m, 4H, CH$_2$P^M), −7.09 (dq, $J_{H,PA}$ = 187.2 Hz, $J_{H,PM}$ = 7.8 Hz, $J_{H,Rh}$ = 7.8 Hz, 1H, Rh–H). ^{31}P{^{1}H} NMR (162 MHz, CD_2Cl_2, 25 ºC): δ 43.8 (dd, $J_{P,Rh}$ = 114, $J_{P,P}$ = 21 Hz, 2P, P^M), 1.3 (dt, $J_{P,Rh}$ = 73, $J_{P,P}$ = 21 Hz, 1P, P^A). MS (MALDI-TOF$^+$): *m/z* (%): 789 (100) [(PhBP$_3$)Rh(H)]$^+$. Anal. Calcd (%) for $C_{49}H_{48}N_2B_2F_4P_3Rh$ (958.36): C 61.41, H 5.05, N 2.92; found: C 61.16, H 5.15, N 2.83. Λ_M (5.0 x 10^{-4} in acetone) = 91.5 S mol^{-1} cm^{-1}.

[(PhBP$_3$)Rh(η^1-C$_2$H$_5$)(κ^2-O$_2$CPh)] (7). A Schlenk tube was charged with solid **1** (75.2 mg, 0.080 mmol) and benzoic acid (9.8 mg, 0.080 mmol) and then toluene (3 mL) was added. The resulting suspension was stirred for two hours under an atmosphere of ethylene. Hexane (10 mL) was added to the pale-yellow suspension to complete the precipitation of the solid, which was filtered, washed with cold hexane (2 x 5 mL) and vacuum-dried. Yield: 56 mg (75 %). IR (solid): ν(CO_2)/cm^{-1}: 1513 (m), 1430 (s). ^{1}H NMR (300 MHz, CD_2Cl_2, −40 ºC): δ 7.98 (d, J = 8.6 Hz, 2H, O$_2$CPh^{o}), 7.92 (m, 4H, Ph$_2{}^{o1}$P^M), 7.68 (d, J = 6.9 Hz, 2H, BPh^{o}), 7.58 (t, J = 8.6 Hz, 1H, O$_2$CPh^{p}), 7.48 (td, J = 11.0, 7.6 Hz, 2H, O$_2$CPh^{m}),

7.33 (m, 8H, BPh^{m} + Ph$_2$^{m1}P^{M} + Ph$_2$^{p2}P^{M}), 7.14 (m, 5H, BPh^{p} + Ph$_2$^{m2}P^{M}), 6.99 (m, 12H, Ph$_2$^{o}P^{A} + Ph$_2$^{o2}P^{M} + Ph$_2$^{p}P^{A} + Ph$_2$^{p1}P^{M}), 6.71 (t, J = 7.0 Hz, 4H, Ph$_2$^{m}P^{A}), 1.76 (br, δ_A, 2H) and 1.49 (br, δ_B, 2H; CH$_2$P^{M}), 1.54 (m, 2H, C*H*$_2$CH$_3$), 1.14 (d, $J_{H,P}$ = 11.5 Hz, 2H, CH$_2$P^{A}), 0.87 (dt, $J_{H,P}$ =11.1 Hz, J = 7.4 Hz, 3H, CH$_2$C*H*$_3$). ^{31}P{^{1}H}NMR (121 MHz, CD_2Cl_2, –40 ºC): δ 36.7 (dd, $J_{P,Rh}$ = 130, $J_{P,P}$ = 23 Hz, 2P, P^{M}), 2.9 (dt, $J_{P,Rh}$ = 67, $J_{P,P}$ = 23 Hz, P^{A}). ^{13}C{^{1}H}NMR (75 MHz, CD_2Cl_2, –40 ºC): δ 179.9 (br s, O$_2$*C*Ph), 32.5 (br d, $J_{C,P}$ = 91 Hz, *C*H$_2$CH$_3$), 15.2 (d, $J_{C,P}$ = 4 Hz, CH$_2$*C*H$_3$). MS (MALDI-TOF$^+$): *m/z* (%): 909 (5) [(PhBP$_3$)Rh(O$_2$CPh)]$^+$, 789 (100) [(PhBP$_3$)Rh(H)]$^+$. Anal. Calcd (%) for $C_{54}H_{51}BO_2P_3Rh$ (938.22): C 69.10, H 5.48; found: C 68.94, H 5.67.

[(PhBP$_3$)Rh(η^1-C$_2$H$_5$)(κ^2-O$_2$CMe)] (8). To a suspension of **1** (110.0 mg, 0.117 mmol) in toluene (2 mL), acetic acid (6.7 μL, 0.117 mmol) was added. The resulting suspension was stirred for two hours under an ethylene atmosphere and the product was isolated as described above for **7**. Yield: 67.0 mg (65 %). IR (solid): ν(CO$_2$)/cm^{-1}: 1521 (m), 1462 (s). ^{1}H NMR (400 MHz, CD_2Cl_2, –40 ºC): δ 7.72 (m, 4H, Ph$_2$^{o1}P^{M}), 7.62 (d, J = 7.0 Hz, 2H, BPh^{o}), 7.41 (t, J = 7.3 Hz 2H, Ph$_2$^{p1}P^{M}), 7.31 (t, J = 7.4 Hz, 2H, BPh^{m}), 7.24 (m, 6H, Ph$_2$^{m1}P^{M} + Ph$_2$^{p2}P^{M}), 7.11 (t, J = 7.0 Hz, 1H, BPh^{p}), 7.07 (m, 10H, Ph$_2$^{m2}P^{M} + Ph$_2$^{o}P^{A} + Ph$_2$^{p}P^{A}), 6.88 (m, 8H, Ph$_2$^{m}P^{A} + Ph$_2$^{o2}P^{M}), 2.03 (s, 3H, O$_2$CCH$_3$), 1.67 (br, δ_A, 2H) and 1.40 (br, δ_B, 2H; CH$_2$P^{M}), 1.52 (m, 2H, C*H*$_2$CH$_3$), 1.33 (d, $J_{H,P}$ = 11.6 Hz, 2H, CH$_2$P^{A}), 0.87 (m, 3H, CH$_2$C*H*$_3$). ^{31}P{^{1}H} NMR (162 MHz, CD_2Cl_2, –40 ºC) δ 36.4 (dd, $J_{P,Rh}$ = 131 Hz, $J_{P,P}$ = 23 Hz, 2P, P^{M}), 3.4 (dt, $J_{P,Rh}$ = 65 Hz, $J_{P,P}$ = 23 Hz, 1P, P^{A}). ^{13}C{^{1}H} NMR (101 MHz, CD_2Cl_2, –40 ºC) from ^{1}H,^{13}C-hsqc and ^{1}H,^{13}C-hmbc spectra δ 185.9 (O$_2$*C*CH$_3$), 31.1 (*C*H$_2$CH$_3$), 25.3 (O$_2$C*C*H$_3$), 14.8 (CH$_2$*C*H$_3$). MS (MALDI-TOF$^+$): *m/z* (%): 847 (47) [(PhBP$_3$)Rh(O$_2$CCH$_3$)]$^+$, 789 (100) [(PhBP$_3$)Rh(H)]$^+$. Anal. Calcd (%) for $C_{49}H_{49}BO_2P_3Rh$ (876.55): C 67.14, H 5.63; found: C 67.17, H 5.57.

[(PhBP$_3$)Rh(H)(κ^2-O$_2$CMe)] (10). Acetic acid (5.2 μL, 0.090 mmol) was added to a solution of [(PhBP$_3$)Rh(H)$_2$(NCMe)] (**3**) (75.0 mg, 0.090 mmol) in toluene (3 mL). After stirring for 20 min, the solution was layered with hexane (10 mL) and left to stand for one day. The pale-yellow solid deposited was washed with hexane (3 x 3 mL) and vacuum-dried. Yield: 61.4 mg (80 %). IR (solid):

ν(Rh–H)/cm^{-1}: 1967 (m), ν(CO_2)/cm^{-1}: 1519 (m), 1457 (s). ^{1}H NMR (300 MHz, C_6D_6, 25 ºC): δ 8.06 (d, J = 7.2 Hz, 2H, BPh^o), 7.84 (m, 4H, $Ph_2^{o1}P^M$), 7.70 (m, 6H, $Ph_2^{o2}P^M$ + BPh^m), 7.43 (br t, J = 7.3Hz, 1H, BPh^p), 7.34 (br t, J = 8.6 Hz, 4H, $Ph_2^oP^A$), 6.89 (m, 8H, $Ph_2^{m1}P^M$ + $Ph_2^{p1}P^M$ + $Ph_2^pP^A$), 6.80 (br t, J = 7.5 Hz, 4H, $Ph_2^mP^A$), 6.67 (m, 6H, $Ph_2^{m2}P^M$ + $Ph_2^{p2}P^M$), 1.92 (s, 3H, O_2CCH_3), 1.80 (br d, J = 12.3 Hz, 2H, CH_2P^A), 1.69 (m, 4H, CH_2P^B), –4.97 (ddd, $J_{H,P}{}^B$ = 193.2 Hz, $J_{H,Rh}$ = 11.7Hz, $J_{H,P}{}^A$ = 9.0 Hz, 1H, Rh–H). ^{31}P{^{1}H} NMR (121 MHz, C_6D_6 , 25 ºC) δ 51.6 (dd, $J_{P,Rh}$ = 123 Hz, $J_{P,P}$ = 20 Hz, 2P, P^M), 8.2 (dt, $J_{P,Rh}$ = 74 Hz, J_{P-P} = 20 Hz, 1P, P^A). ^{13}C{^{1}H}NMR (75 MHz, C_6D_6, 25 ºC) from ^{1}H,^{13}C-hsqc and ^{1}H,^{13}C-hmbc spectra δ 185.3 (O_2CCH_3), 24.3 (O_2CCH_3). MS (MALDI-TOF$^+$): *m/z* (%):789 (100) [(PhBP$_3$)Rh(H)]$^+$. Anal. Calcd (%) for $C_{47}H_{45}BO_2P_3Rh$ (848.50): C 66.53, H 5.35; found: C 65.58, H 5.25.

[{PhB(PMe)P$_2$}Rh(κ^2-O$_2$SOCF$_3$)] (11). Addition of MeO_3SCF_3 (MeOTf, 2.5 μL, 0.023 mmol) to a solution of **1** (21.6 mg, 0.023 mmol) in CD_2Cl_2 (0.5 mL) caused the almost immediate discoloration of the solution from orange to pale-yellow. NMR data indicated the formation of complex **12** in 80 % yield. Selected spectroscopic data: ^{1}H NMR (300 MHz, CD_2Cl_2, 25 ºC): δ 7.9-6.9 (35H, Ph), 4.06 (d, $J_{H,P}$ =12.4 Hz, 2H, CH_2P^M), 2.81 (d, $J_{H,P}$ =12.9 Hz, 3H, CH_3P^M), 1.55 (br, 4H, CH_2P^A). ^{31}P{^{1}H}NMR (121 MHz, CD_2Cl_2, 25 ºC): δ 74.8 (s, 1P, P^M), 34.1 (d, $J_{P,Rh}$ = 110, 2P, P^A).

[{(PhBP$_3$)Rh}$_2$(μ-Cl)$_3$]OTf ([12]$^+$). To a solution of [(PhBP$_3$)Rh(Cl)$_2$] (50.3 mg, 0.059 mmol) in dichloromethane (2 mL), MeOTf (3.2 μL, 0.029 mmol) was added. After stirring for 6 h at room temperature the orange solution was carefully layered with diethyl ether (10 mL) and maintained undisturbed for two days. The yellow-orange microcrystals deposited were decanted, washed with diethyl ether (2 x 3 mL) and vacuum-dried. Yield: 40.0 mg (75 %). ^{1}H NMR (300 MHz, C_6D_6, 25 ºC): δ 7.64 (d, J = 7.3 Hz, 4H, BPh^o), 7.32 (m, 24H, Ph_2^oP), 7.30 (t, J = 7.4 Hz, 4H, BPh^m), 7.17 (t, J = 7.6 Hz, 12H, Ph_2^pP), 7.07 (m, 26H, Ph_2^mP + BPh^p), 1.45 (br d, $J_{H,P}$ = 7.0 Hz, 12H, CH_2P). ^{31}P{^{1}H}NMR (121 MHz, CD_2Cl_2, 25 ºC): δ 33.5 (d, $J_{P,Rh}$ = 110 Hz, 6P). MS (MALDI-TOF$^+$): *m/z* (%): 823 (100)

$[(PhBP_3)Rh(Cl)]^+$. Anal. Calcd (%) for $C_{91}H_{82}B_2Cl_3F_3O_3P_6SRh_2 \cdot 2CH_2Cl_2$ (2002.18): C 55.79, H 4.33, S 1.60; found: C 55.69, H 4.20, S 1.49.

Reaction of $[(PhBP_3)Rh(H)(NCMe)_2]BF_4$ ($[6]^+$) with PPNCl. $HBF_4 \cdot Et_2O$ (2.0 μL, 0.014 mmol) and acetonitrile (2 μL) were added to a solution of **1** (13.1 mg, 0.014 mmol) in CD_2Cl_2 at −50 ºC. The quantitative formation of $[\mathbf{6}]^+$ was observed by ^1H NMR. Addition of PPNCl (8.0 mg, 0.014 mmol) at room temperature causes the replacement of acetonitrile and formation of the *cis*/*trans* isomers of $[\{(PhBP_3)Rh(H)(\mu\text{-}Cl)\}_2]$, identified by comparison of the NMR data with those previously reported.[19]

Reaction of $[(PhBP_3)Rh(NCMe)_3](PF_6)_2$ ($[2]^+$) with PPNCl. PPNCl (8.6 mg, 0.015 mmol) was added to a solution of $[(PhBP_3)Rh(NCMe)_3](PF_6)_2$ ($[\mathbf{2}]^+$) (12.0 mg, 0.010 mmol) in CD_2Cl_2 (0.5 mL). After stirring for 10 min, the $^{31}P\{^1H\}$ NMR spectrum showed a sole doublet at δ 33.5 ppm ($J_{P,Rh}$ = 110 Hz) corresponding to $[\{(PhBP_3)Rh\}_2(\mu\text{-}Cl)_3]^+$ while other intermediates were not detected. A further addition of PPNCl (3.0 mg, 0.005 mmol) caused the complete transformation of $[\{(PhBP_3)Rh\}_2(\mu\text{-}Cl)_3]^+$ into the neutral $[(PhBP_3)Rh(Cl)_2]$ according to the single doublet at δ 52.2 ppm ($J_{P,Rh}$ = 109 Hz) in the $^{31}P\{^1H\}$ NMR spectrum, which does not evolve further to anionic species of the type $[(PhBP_3)Rh(Cl)_3]^-$ in the presence of an excess of PPNCl.

DFT geometry optimizations. The computational method used was density functional theory (DFT) with the B3LYP exchange-correlation functional,[41] using the Gaussian 09[42] program package. The basis sets used for the full optimization of the structure were LanL2DZ effective core potential for the rhodium atom, and 6-31G(d,p) for the remaining atoms.

X-ray diffraction studies on **1**·2($NCCH_3$), **[2]**$(BF_4)_2$·3(C_6D_6), **4**·2(C_6H_6) and **5**·C_7H_8·C_6H_{14}. Selected crystallographic data for these complexes can be found in Table 5. Intensity measurements were collected with a Smart Apex diffractometer, with graphite-monochromated MoK_α radiation. A semi-empirical absorption correction was applied to each data set, with the multi-scan[43] methods. All non-hydrogen atoms were refined with anisotropic displacement parameters except those atoms involved in disorders which were refined with isotropic displacement parameters: a phenyl ring and an acetonitrile

solvent molecules in **1**·2($NCCH_3$), one benzene solvent molecule in [**2**](BF_4)$_2$·3(C_6D_6), and one hexane solvent molecule in **5**·(C_7H_8)·(C_6H_{14}). The hydrogen atoms were placed at calculated positions and were refined isotropically in riding mode, with the exception of the hydride ligands which were found on the difference-Fourier maps and refined with some constraints. The structures were solved by the Patterson method and refined by full-matrix least-squares with the program SHELX97[44] in the WINGX[45] package.

Table 5. Selected crystal, measurement and refinement data for compounds **1**·2($NCCH_3$), **[2]**(BF_4)$_2$·3(C_6D_6), **4**·2(C_6H_6) and **5**·C_7H_8·C_6H_{14}.

	1·2($NCCH_3$)	**[2]**(BF_4)$_2$·3(C_6D_6)	**4**·2(C_6H_6)	**5**·C_7H_8·C_6H_{14}
Formula	$C_{49}H_{48}BNP_3Rh$·2(C_2H_3N)	$C_{51}H_{50}B_3F_8N_3P_3Rh$·3($C_6D_6$)	$C_{90}H_{86}B_2P_6Rh_2$·2(C_6H_6)	$C_{90}H_{85}B_2P_6Rh_2$·C_7H_8·C_6H_{14}
formula weight	939.62	1337.55	1737.06	1758.15
Colour	orange	colourless	orange	red
crystal system	Monoclinic	Triclinic	Triclinic	Triclinic
space group	$P2_1/n$	P-1	P-1	P-1
a[Å]	15.7452(16)	12.9713(10)	12.435(2)	13.276(4)
b[Å]	13.4974(14)	13.0463(10)	12.972(2)	13.764(4)
c[Å]	21.886(2)	19.7923(15)	14.316(3)	26.816(8)
α[º]	90	80.6362(10)	91.630(2)	99.910(4)
β[º]	93.482(2)	76.7235(10)	100.044(2)	94.923(4)
γ[º]	90	79.7700(10)	114.017(2)	116.112(6)
V[Å^3]	4642.6(8)	3182.0(4)	2064.4(6)	4261(2)
Z	4	2	1	2
F(000)	1952	1360	900	1830
ρ_{calcd}[g cm^{-3}]	1.344	1.396	1.397	1.370
μ (mm^{-1})	0.511	0.411	0.566	0.549
crystal size[mm]	0.09 × 0.06 × 0.05	0.20 × 0.19 × 0.14	0.10 × 0.08 × 0.03	0.20 × 0.15 × 0.08
temperature [K]	100(2)	100(2)	100(2)	100(2)
θ limits [º]	25.25	27.00	25.20	27.00
collected reflns.	25414	37706	15838	49931
unique reflns. (Rint)	8380 (0.1011)	13826 (0.0442)	7382 (0.0634)	18459 (0.0503)
reflns. with $I>2\sigma(I)$	5673	10289	5082	15482

parameters/restraints	548/10	747/0	509/2	1012/33
R_1 (on F, I>2σ(I))	0.0751	0.0438	0.0512	0.0481
wR_2 (on F^2, all data)	0.1433	0.1111	0.1221	0.1152
max./min. Δρ [e Å^{-3}]	0.659/-0.711	0.846/–0.568	0.790/–1.159	0.981/–0.711
goodness of fit	1.060	1.025	0.985	1.091

Supporting Information Available. Full ORTEP diagrams, selected spectroscopic data, DOSY experiments, atomic coordinates for **1'**, complete reference 41, and a CIF file giving details of the X-ray crystal structures of **1**·2($NCCH_3$), **[2](BF_4)$_2$**·3(C_6D_6), **4**·2(C_6H_6) and **5**·C_7H_8·C_6H_{14}. This material is available free of charge via the Internet at http://pubs.acs.org.

Acknowledgments. This research was supported by the MICINN/FEDER (Projects CTQ2008-03860 and CTQ2011-22516, Spain) and Gobierno de Aragón (Group E70, Spain). A. G. and S. J. thank Gobierno de Aragón for a fellowship.

Dedication. This article is dedicated to the memory of Prof. F. Gordon A. Stone, a pioneer that devoted his whole life to chemistry and lent a hand to some of us to take the first steps in organometallic chemistry.

References

(1) See for example: (a) Paneque, M.; Poveda, M. L.; Rendón, N. *Eur. J. Inorg. Chem.* **2011**, 19–33. (b) Dias, H. V. R.; Lovely, C. J. *Chem. Rev.* **2008**, *108*, 3223–3238. (c) Lail M.; Pittard, K. A.; Gunnoe T. B. *Adv. Organomet. Chem.* **2008**, *56*, 95–153. (d) Becker, E.; Pavlik, S.; Kirchner, K. *Adv. Organomet. Chem.* **2008**, *56*, 155–197. (e) Crossley I. R. *Adv. Organomet. Chem.* **2008**, *56*, 199–321. (f) Trofimenko, S. *Polyhedron* **2004**, *23*, 197–203. (g) Pettinari, C.; Santini, C. in *Comprehensive Coord. Chem. II*, McCleverty, J. A. and Meyer, T. J. Eds; Elsevier Pergamon: Oxford, **2004**, Vol. 1, Ch. 1.10,

pp. 159–210. (h) Slugovc, C.; Padilla-Martinez, I.; Sirol, S.; Carmona, E. *Coord. Chem. Rev.* **2001**, *213*, 129–157. (i) Trofimenko, S. *Scorpionates: The Coordination Chemistry of Polypyrazolylborate Ligands*, Imperial College Press: London, **1999**.

(2) (a) Smith, J. M. *Comments Inorg. Chem.* **2008**, *29*, 189–233. (b) Stradiotto, M.; Hesp, K. D.; Lundgren, R. J. *Angew. Chem., Int. Ed*. **2010**, *49*, 494–512.

(3) (a) Peters, J. C.; Feldman, J. D.; Tilley, T. D. *J. Am. Chem. Soc.* **1999**, *121*, 9871–9872. (b) Barney, A. A.; Heyduk, A. F.; Nocera, D. G. *Chem. Commun.* **1999**, 2379–2380.

(4) (a) Jenkins, D. M.; Peters, J. C. *J. Am. Chem. Soc.* **2005**, *127*, 7148–7165. (b) Brown, S. D.; Peters, J. C. *J. Am. Chem. Soc.* **2005**, *127*, 1913–1923. (c) MacBeth, C. E.; Thomas, J. C.; Betley, T. A.; Peters, J. C. *Inorg. Chem.* **2004**, *43*, 4645–4662. (d) Jenkins, D. M.; Peters, J. C. *J. Am. Chem. Soc.* **2003**, *125*, 11162–11163. (e) Turculet, L.; Feldman, J. D.; Tilley, T. D. *Organometallics* **2003**, *22*, 4627–4629.

(5) (a) Mehn, M. P.; Brown, S. D.; Jenkins, D. M.; Peters, J. C.; Que Jr., L. *Inorg. Chem.* **2006**, *45*, 7417–7427. (b) Brown, S. D.; Betley, T. A.; Peters, J. C. *J. Am. Chem. Soc.* **2003**, *125*, 322–323. (c) Jenkins, D. M.; Betley, T. A.; Peters, J. C. *J. Am. Chem. Soc.* **2002**, *124*, 11238–11239. (d) Jenkins, D. M.; Di Bilio, A. J.; Allen, M. J.; Betley, T. A.; Peters, J. C. *J. Am. Chem. Soc.* **2002**, *124*, 15336–15350.

(6) Tejel, C.; Ciriano, M. A.; Jiménez, S.; Passarelli, V.; López, J. A. *Angew. Chem. Int. Ed.* **2008**, *47*, 2093–2096.

(7) Hou, H.; Rheingold, A. L.; Kubiak, C. P. *Organometallics* **2005,** *24,* 231–233.

(8) Feldman, J. D.; Peters, J. C.; Tilley, T. D. *Organometallics* **2002**, *21*, 4050–4064.

(9) (a) Feldman, J. D.; Peters, J. C.; Tilley, T. D. *Organometallics* **2002**, *21*, 4065–4075.

(10) (a) Brown, S. D.; Mehn, M. P.; Peters, J. C. *J. Am. Chem. Soc.* **2005**, *127*, 13146–13147. (b) Brown, S. D.; Peters, J. C. *J. Am. Chem. Soc.* **2004**, *126*, 4538–4539.

(11) Thomas, C. M.; Peters, J. C. *Angew. Chem. Int. Ed.* **2006**, *45*, 776–780.

(12) Turculet, L.; Feldman, J. D.; Tilley, T. D. *Organometallics* **2004,** *23,* 2488–2502.

(13) (a) Betley, T. A.; Peters, J. C. *J. Am. Chem. Soc.* **2004**, *126*, 6252–6254. (b) Betley, T. A.; Peters, J. C. *J. Am. Chem. Soc.* **2003**, *125*, 10782–10783.

(14) Lu, C. C.; Peters, J. C. *Inorg. Chem.* **2006**, *45*, 8597–8607.

(15) Thomas, C. M.; Mankad, N. P.; Peters, J. C. *J. Am. Chem. Soc.* **2006**, *128*, 4956–4957.

(16) (a) Camerano, J. A.; Casado, M. A.; Ciriano, M. A.; Tejel, C.; Oro, L. A. *Chem Eur. J.* **2008**, 14, 1897–1905. (b) Casado, M. A.; Hack, V.; Camerano, J. A.; Ciriano, M. A.; Tejel, C.; Oro, L. A. *Inorg. Chem.* **2005**, *44*, 9122–9124.

(17) Daida, E. J.; Peters J. C. *Inorg. Chem.* **2004**, *43*, 7474–7485.

(18) Betley, T. A. Peters, J. C. *Inorg. Chem.* **2003**, *42*, 5074–5084.

(19) Jiménez, S.; López, J. A.; Ciriano, M. A.; Tejel, C.; Martínez, A.; Sánchez-Delgado, R. A. *Organometallics* **2009,** *28,* 3193–3202.

(20) Walker, J. M.; Cox, A. M.; Wang, R.; Spivak, G. J. *Organometallics* **2010**, *29*, 6121–6124.

(21) Tejel, C.; Ciriano, M. A., Passarelli, V. *Chem. Eur. J.* **2011**, *17*, 91–95.

(22) Nicasio, M. C.; Paneque, M.; Pérez, P. J.; Pizzano, A.; Poveda, M. L.; Rey, L.; Sirol, S.; Taboada, S.; Trujillo, M.; Monge, A.; Ruiz, C.; Carmona, E. *Inorg. Chem.* **2000**, *39*, 180–188.

(23) Paneque, M.; Pérez, P. J.; Pizzano, A.; Poveda, M. L.; Taboada, S.; Trujillo, M.; Carmona, E. *Organometallics* **1999**, *18*, 4304–4310.

(24) (a) Beach, M. T.; Walker, J. M.; Larocque, T. G.; Deagle, J. L.; Wang, R.; Spivak, G. J. *J. Organomet. Chem.* **2008**, *693*, 2921–2928. (b) Thomas, J. C.; Peters, J. C. *Polyhedron* **2004**, *23*, 489–497. (c) Thomas, C. M.; Peters, J. C. *Inorg. Chem.* **2004**, *43*, 8–10.

(25) Bianchini, C.; Farnetti, E.; Graziani, M.; Kaspar, J. Vizza, F. *J. Am. Chem. Soc.* **1993**, *115,* 1753–1759.

(26) Hanke, D.; Wieghardt, K.; Nuber, B.; Lu, R.-S.; McMullan, R. K.; Koetzle, T. F.; Bau, R. *Inorg. Chem.* **1993**, *32*, 4300–4305.

(27) Bianchini, C.; Meli, A.; Laschi, F.; Ramirez, J. A.; Zanello, P.; Vacca, A. *Inorg. Chem.* **1988,** *27*, 4429–4435.

(28) See for example: (a) $[\{(PhBP_3)Ir(H)(\mu\text{-}H)\}_2]$ (Ir–Ir, 2.797(2) Å, ref. 8). (b) $[\{(N_2P)Ir(H)(\mu\text{-}H)\}_2]^{2+}$ (N_2P = bis(oxazoline)phosphonite, Ir–Ir, 2.7651(5) Å): Peloso, R.; Pattacini, R.; Cazin, C. S. J.; Braunstein, P. *Inorg. Chem.* **2009**, *48*, 11415–11424. (c) $[\{(PPhMe_2)_2Ir(H)_2(\mu\text{-}H)\}_2]^{2+}$ (Ir–Ir, 2.739(1) Å): Robertson, G. B.; Tucker, P. A. *Aust. J. Chem.* **1984**, *37*, 257–263. (d) $[\{(L_2)Ir(H)_2(\mu\text{-}H)\}_2]^{2+}$ (L_2 = $(C_2F_5)_2PCH_2CH_2(C_2F_5)_2$, Ir–Ir, 2.703(2) Å): Schnabel, R. C.; Carroll, P. S.; Roddick, D. M. *Organometallics* **1996,** *15,* 655–662. (e) $[\{(\kappa^2\text{-}L_3)Ir(H)_2(\mu\text{-}H)\}_2]^{2+}$ (L_3 = $^tBu_2PC_2H_4NHC_2H_4NEt_2$, Ir–Ir, 2.73 Å): Choualeb, A.; Lough, A. L.; Gusev, D. G. *Organometallics* **2007,** *26,* 5224–5229.

(29) (a) Bianchini, C.; Laschi, F.; Masi, D.; Mealli, C.; Meli, A.; Ottaviani, F. M.; Proserpio, D. M.; Sabat, M.; Zanello, P. *Inorg. Chem.* **1989,** *28,* 2552–2560. (b) Bianchini, C.; Mealli, C.; Meli, A.; Sabat, M. *J. Chem. Soc., Chem. Commun.*, **1986**, 777–779.

(30) Several cationic $[\{(Cp^*)Ir\}_2(\mu\text{-}H)_3]X$ complexes with different counteranions have been described: (a) Ogo, S.; Nakai, H.; Watanabe, Y. *J. Am. Chem. Soc.* **2002**, *124*, 597–601 (X = NO_3, Ir–Ir, 2.4677(4) Å). (b) Hou, Z.; Koizumi, T.; Fujita, A.; Yamazaki, H.; Wakatsuki, Y. *J. Am. Chem. Soc.* **2001,** *123,* 5812–5813 (X = 2-(2'-hydroxyphenyl)phenoxide, Ir–Ir, 2.4740(10) Å). (c) Stevens, R. C.; Mclean, M. R.; Wen, T.; Carpenter, J. D.; Bau, R.; Koetzle, T. F. *Inorg. Chim. Acta* **1989**, *161*, 223–231 (X = ClO_4, Ir–Ir, 2.465(3) Å). (d) Bau, R.; Teller, R. G.; Kirtley, S. W.; Koetzle, T. F. *Acc. Chem. Res.* **1979**, *12*, 176–183 (X = BF_4, Ir–Ir, 2.458 (6) Å).

(31) H_2 was identified by ^1H NMR spectroscopy as a sharp singlet at δ 4.45 ppm (C_6D_6) and 4.60 ppm (CD_2Cl_2).

(32) (a) Besora, M.; Lledós, A.; Maseras, F. *Chem. Soc. Rev.* **2009**, *38*, 957–966, *and references therein*. (b) Morris, R. H. *Coord. Chem. Rev.* **2008**, *252*, 2381–2394. (c) Heinekey, D. M.; Oldham, W. J. *Chem. Rev.* **1993**, *93*, 913–926. (d) Jessop, P. G.; Morris, R. H. *Coord. Chem. Rev.* **1992**, *121*, 155–284.

(33) See for example: (a) Åkermark, B.; Martin, J.; Nyström, J.–E.; Strömberg, S.; Svensson, M.; Zetterberg, K.; Zuber, M. *Organometallics* **1998**, *17*, 5367–5373. (b) Henderson, R. A.; Oglieve, K. E. *J. Chem. Soc., Chem. Commun*. **1991**, *18*, 584–586. (c) Green, M.; Grove, D. M.; Spencer, J. L.; Stone, F. G. A. *J. Chem. Soc. Dalton Trans.* **1977**, 2228–2234. (d) Evans, J.; Johnsson, B. F. G.; Lewis, J. *J. Chem. Soc. Chem. Commun.* **1971**, 1252–1253.

(34) See for example: (a) Findlater, M.; Cartwright-Sykes, A.; White, P, S.; Schauer, C. K.; Brookhart, M *J. Am. Chem. Soc*. **2011**, *133*, 12274–12284. (b) Frech, C. M.; Shimon, L. J. W.; Milstein, D. *Organometallics*, **2009**, *28,* 1900–1908. (c) Shiotsuki, M.; White, P. S.; Brookhart, M.; Templeton, J. L. *J. Am. Chem. Soc*. **2007**, *129*, 4058–4067. (d) Tejel, C.; Ciriano, M. A.; Millaruelo, M.; López, J. A.; Lahoz, F. J.; Oro, L. A. *Inorg. Chem.* **2003**, *42*, 4750–4758. (e) de Bruin, B.; Boerakker, M. J.;

Verhagen, J. A. W.; de Gelder, R.; Smits, J. M. M.; Gal, A. W. *Chem. Eur. J.* **2000**, *6*, 298–312. (f) Wang, D.; Angelici, R. J. *Inorg. Chem.* **1996**, *35*, 1321–1331. (g) Brookhart, M.; Hauptman, E.; Lincoln, D. M. *J. Am. Chem. Soc.* **1992**, *114*, 10394–10401. (h) Bennett, M. A.; McMahon, I. J.; Pelling, S.; Brookhart, M.; Lincoln, D. M. *Organometallics* **1992**, *11*, 127–138. (i) Mole, L.; Spencer, J. L.; Carr, N.; Orpen, A. G. *Organometallics* **1991**, *10*, 49–52.

(35) Öhrström, L.; Strömberg, S.; Glaser, J.; Zetterberg, K.; *J. Organomet. Chem.* **1998**, *558*, 123–130, *and references therein*.

(36) Henderson, R. A. *Angew. Chem. Int. Ed. Engl.* **1996**, *33*, 947–967.

(37) Tejel, C.; Ciriano, M. A.; López, J. A.; Lahoz, F. J.; Oro, L. A. *Organometallics* **1997**, *16*, 4718–4727.

(38) (a) Suzuki, T.; Isobe, K.; Kashiwabara, K.; Fujita, J.; Kaizaki, S. *J. Chem. Soc., Dalton Trans.* **1996**, 3779–3786. (b) Bachechi, F. *Acta Cryst.* **1994**, C*50*, 1069–1072.

(39) Perrin, D. D. W.; Armarego, L. F. Purification of Laboratory Chemicals, 3rd ed., Pergamon Press, Exeter, UK 1988.

(40) Cramer, R. *Inorg. Chem.* **1962**, *1*, 722–723.

(41) (a) Becke, A. D. *Phys. Rev. A*, **1988**, *38*, 3098–3100. (b) Lee, C.; Yang, W.; Parr, R. G. *Phys. Rev. B*, **1988**, *37*, 785–789. (c) Becke, A. D. *J. Chem. Phys.* **1993**, *98*, 5648–5652.

(42) Gaussian 09, Revision A.02, Frisch, M. J.; et al., Gaussian, Inc., Wallingford CT, **2009**. (see Supporting Information for complete citation).

(43) Sheldrick, G. M. SADABS, Bruker AXS, Madison, WI (USA), 1997.

(44) Sheldrick, G. M. *Acta Cryst.* **2008**, *A64*, 112–122.

(45) Farrugia, L. F. *J. Appl. Crystallogr.* **1999**, *32*, 837–838.

Figure for the Table of Contents